High Temperature Corrosion of Fe Coated with a $(Li_{0.62}K_{0.38})_2CO_3$ Melt

Baek-un KIM, Hideaki YOSHITAKE, Harumi YOKOKAWA,† Nobuyuki KAMIYA, and Ken-ichiro OTA*
Department of Energy Engineering, Yokohama National University, 156 Tokiwadai, Hodogaya-ku, Yokohama 240
† National Chemical Laboratory for Industry, Tsukuba Research Center, Ibaraki 305

(Received November 30, 1992)

The corrosion of Fe in the presence of $(Li_{0.62}K_{0.38})_2CO_3$ has been studied under an O_2/CO_2 atmosphere at 823—1073 K by TGA. The corrosion of Fe coated with a $(Li_{0.62}K_{0.38})_2CO_3$ melt obeyed the parabolic rate law, and $LiFeO_2$ and $LiFe_5O_8$ were formed. Under these conditions severe corrosion did not occur because of the low solubility of iron oxide in the melt. When Fe was immersed in $(Li_{0.62}K_{0.38})_2CO_3$, the reaction obeyed the linear rate law and Li_5FeO_4, $LiFeO_2$, and $LiFe_5O_8$ were formed. This was in accordance with the thermochemical phase study. Li_5FeO_4 was mostly formed during the intitial period of the corrosion reaction and caused a weight decrease of the reaction cell (specimen+melt) by the liberation of CO_2. $LiFe_5O_8$ was formed in the later period of the reaction.

The molten carbonate fuel cell (MCFC) is favored for the fact that a wide variety of fuels, such as hydrogen, hydrocarbons, carbon monoxide, and their mixtures (coal gas), can be used. The exhaust heat of the MCFC is more valuable than that of the phosphoric acid fuel cell (PAFC), since the operating temperature of the MCFC is higher. The MCFC can be used in cogeneration systems. The MCFC power generation system is expected to be one of the most promising power generation systems for the coming century due to its excellent environmental characteristics.

In this system, the durability of the components of the MCFC is quite important for commercialization. Many metallic materials are used in the MCFC. Current collectors and separators are presently made of stainless steel.

The corrosion of metals coated with molten carbonate has been reported in several papers.[1—5] Shores studied the corrosion behavior of selected alloys with molten carbonate under fuel cell operating conditions.[1] He presented phase diagrams of the Li–Fe–C–O system and the Li–Cr–C–O system, and reported that the corrosion of stainless steels with 1×10^{-2} kg m^{-2} of $(Li_{0.62}K_{0.38})_2CO_3$ coating occurred at a high reaction rate in a reducing gas atmosphere, but in an oxidizing environment the corrosion rate was relatively moderate. He also mentioned the difficulty in understanding the corrosion mechanism due to the complexity of fuel cell environments.

In order to understand the corrosion mechanism of alloys, the corrosion characteristics of each component should be known. Iron is most widely used for metallic materials and is a main component of stainless steels. Thus the study of the corrosion of iron in the presence of molten carbonate is very important in order to understand the corrosion behavior of stainless steels. Azzi reported that the corrosion products of Fe in a $(Na_{0.58}K_{0.42})_2CO_3$ melt under a CO_2/O_2 atmosphere are FeO, Fe_3O_4, and Fe_2O_3.[2] Hsu presented phase diagrams for the Fe–Li–K–C–O systems derived by thermochemical calculations at 923 K.[3] The phase relationships were also checked experimentally by TGA and DTA. The corrosion of iron with 2×10^{-2} kg m^{-2} of $(Li_{0.62}K_{0.38})_2CO_3$ coating under a 20%O_2–(0.001—50)%CO_2–Ar atmosphere at 923 K obeyed the parabolic rate law.

Several corrosion products have been reported for the corrosion of Fe with molten carbonate. They were mostly Fe oxides (FeO, Fe_3O_4, Fe_2O_3) and sometimes contained Li or K. Under $P_{O_2}<10^{-3}$ atm, the corrosion obeyed the linear rate law and the corrosion products were $Li_2Fe_3O_5$ or $LiFe_3O_5+LiFe_5O_8$.[4] We reported the corrosion of iron in the presence of Li_2CO_3 under 33%O_2–67%CO_2 at 1073 K and measured the weight decrease of the cell (specimen+melt), when Fe was immersed in the melt. The weight decrease was caused by the formation of lithium iron oxide with high lithium content such as Li_5FeO_4.[5]

Further study is necessary to understand the corrosion of Fe in the presence of a carbonate melt, especially in relation to temperature dependence and the effect of the atmosphere. In this study, $(Li_{0.62}K_{0.38})_2CO_3$ was selected as a melt since this is the standard melt composition for the MCFC and the corrosion of Fe coated with the melt was studied in a CO_2/O_2 atmosphere at 823—1073 K.

Experimental

Fe specimens (6×10^{-3} m)×(12×10^{-3} m) were cut from a sheet of 99.99% Fe (10^{-3} m thickness, impurities are shown in Table 1) and polished successively with #600—#1500 SiC abrasive papers, followed by degreasing with a neutral detergent, washing with ethanol, drying, and weighing before testing.

For the thin film coating, 0—40×10^{-2} kg m^{-2} of

Table 1. Chemical Composition of Fe Specimen (wt. ppm)

	C	Si	Mn	P	S	Cu	Ni	Cr	O	N
99.99% Fe	10	<20	2	<20	10	6	2	3	360	40

$(Li_{0.62}K_{0.38})_2CO_3$ was coated on the surface of the Fe specimen by dipping into the carbonate–ethanol mixture and drying. The amount of carbonate on the metal was determined by the weight difference of the Fe specimen before and after the coating process. The Fe specimen with carbonate was placed in a gold cell as shown in Fig. 1 (A). For the immersion test, the metal specimen and carbonate were put in a gold cell as shown in Fig. 1 (B).

Before the corrosion test, the specimen was held at 463 K for 20 min in order to remove the remaining moisture. The weight gain of the specimen was measured and monitored continuously by TGA (Shimadzu DT-40). The atmosphere was mainly a $67\%CO_2$–$33\%O_2$ gas mixture with a flow rate of 75×10^{-6} $m^3\,min^{-1}$. To examine the effect of the gas composition, CO_2 and O_2 pressures were varied from 10^{-5} to 0.85 atm and from 0.1 to 0.9 atm, respectively. The reaction temperature was varied from 823 to 1073 K. The reaction time was normally 30—100 h. After the corrosion test, the corrosion products were analyzed by X-ray diffraction. The metal consumption during the corrosion was also determined by weighing, after etching the oxide scale.[6)]

Results and Discussion

Figure 2 shows the weight gain curves for the corrosion of Fe in the presence of $(Li_{0.62}K_{0.38})_2CO_3$ under $33\%O_2$–$67\%CO_2$ at 923 K. With 35×10^{-2} kg m^{-2} of $(Li_{0.62}K_{0.38})_2CO_3$ coating, the weight gain was 14.7×10^{-2} kg m^{-2} after 30 h and was 15% larger than that without melt. The difference was relatively small and accelerated corrosion did not occur. Namely, the effect of a thin film of the carbonate melt on Fe corrosion was smaller than that on Ni corrosion.[7)] This might be caused by the low solubility of iron oxide in $(Li_{0.62}K_{0.38})_2CO_3$.[8)] The solubility of Fe oxide under these conditions is 3×10^{-6} (mole fraction). This value is 1/10 of that of NiO (36×10^{-6} mole fraction). On the other hand, when Fe was immersed in $(Li_{0.62}K_{0.38})_2CO_3$, the weight decreased during an initial period and then increased. This weight decrease will be discussed later.

Figure 3 shows the influence of the amount of coating on the corrosion of Fe coated with $(Li_{0.62}K_{0.38})_2CO_3$ under $33\%O_2$–$67\%CO_2$ at 923 K. All the reactions obeyed the parabolic rate law. The parabolic rate constant increased with increasing amounts of coating up

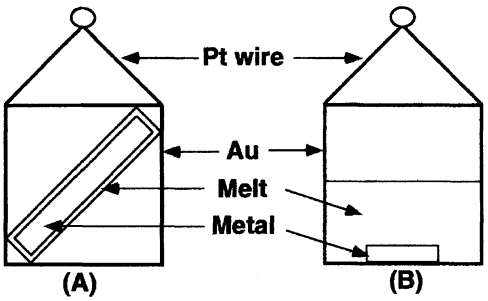

Fig. 1. Schematic drawings of the reaction cells for TGA. (A): coated with melt, (B): immersed in melt.

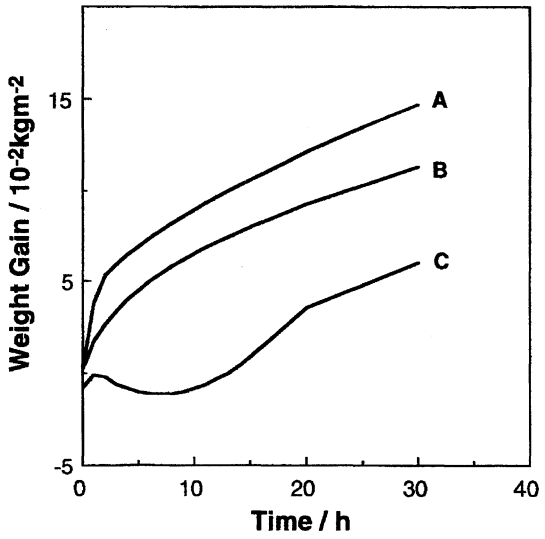

Fig. 2. Weight gain curves for the corrosion of Fe at 923 K under $67\%CO_2$–$33\%O_2$. A: 35×10^{-2} kg m^{-2}, B: without melt, C: immersed in $(Li_{0.62}K_{0.38})_2CO_3$ (Fe/melt=1/1.5).

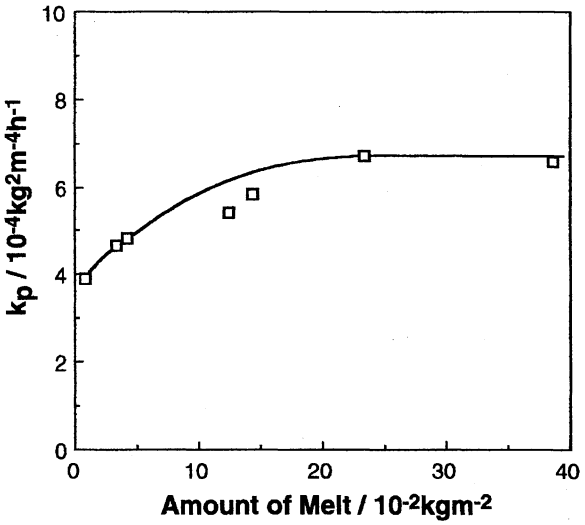

Fig. 3. Parabolic rate constant (k_p) for the corrosion of Fe coated with $(Li_{0.62}K_{0.38})_2CO_3$ at 923 K under $67\%CO_2$–$33\%O_2$.

to 23×10^{-2} kg m^{-2} of $(Li_{0.62}K_{0.38})_2CO_3$ and then became constant above 23×10^{-2} kg m^{-2}. The typical effect of the carbonate melt on the corrosion of metals in which a maximum corrosion rate is observed for about 1×10^{-2} kg m^{-2} coating was not observed in this study. The corrosion rate was independent of the coating amount above 23×10^{-2} kg m^{-2}. This was because the excess melt flowed down to the bottom of the cell and the thickness of the film remained constant owing to the surface tension. In other words, the metal surface could not support more than 23×10^{-2} kg m^{-2} of the carbonate melt. For this reason, the coated amount was mostly fixed at 32×10^{-2} kg m^{-2} in order to study the influence of temperature and atmosphere where good

reproducibility of the reaction was obtained.

Figure 4 shows the weight gain curves for the corrosion of Fe coated with 32×10^{-2} kg m^{-2} of $(Li_{0.62}K_{0.38})_2CO_3$ at 823—1073 K. The reaction obeyed the parabolic rate law and the rate increased with temperature. This tendency is normal and different from that of Ni corrosion. The corrosion rate of Ni with a $(Li_{0.62}K_{0.38})_2CO_3$ coating decreased at higher temperatures owing to the solubility decrease of NiO.[9] Figure 5 shows the Arrhenius plots of the parabolic rate constant (k_p) for the corrosion of Fe with and without $(Li_{0.62}K_{0.38})_2CO_3$. The corrosion rate with a $(Li_{0.62}K_{0.38})_2CO_3$ coating was not much different from that without the melt and the slopes of the lines (activation energy) were almost the same. This tendency may be mainly caused by the low solubility of Fe oxide in the carbonate melt.[8] X-Ray diffraction of the oxide scale of corroded Fe with the $(Li_{0.62}K_{0.38})_2CO_3$ coating at 923—1073 K showed that the corrosion products were FeO, Fe_3O_4, and lithiated iron oxides ($LiFe_5O_8$ and $LiFeO_2$). The oxide scale of Fe without the melt consisted mainly of FeO and Fe_3O_4. In spite of the difference in the corrosion products, the reaction rates were almost same. This means that the rate determining step for both corrosion reactions is the same. Namely, the step might be the diffusion of oxide ions through an Fe_3O_4 layer.[10]

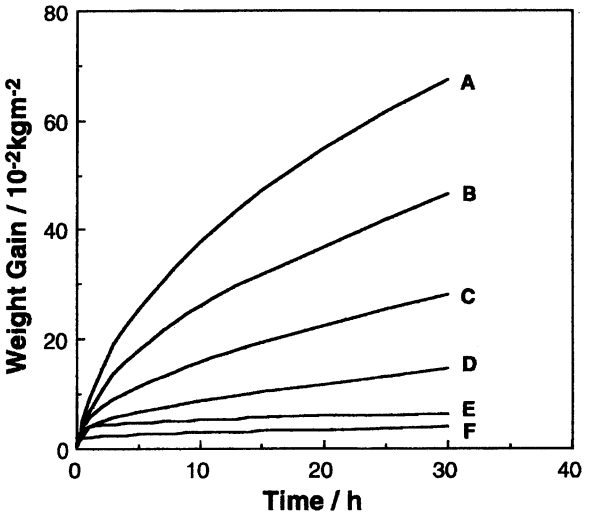

Fig. 4. Weight gain curves for the corrosion of Fe coated with 32×10^{-2} kg m^{-2} of $(Li_{0.62}K_{0.38})_2CO_3$ under $67\%CO_2$–$33\%O_2$. A: 1073 K, B: 1023 K, C: 973 K, D: 923 K, E: 873 K, F: 823 K.

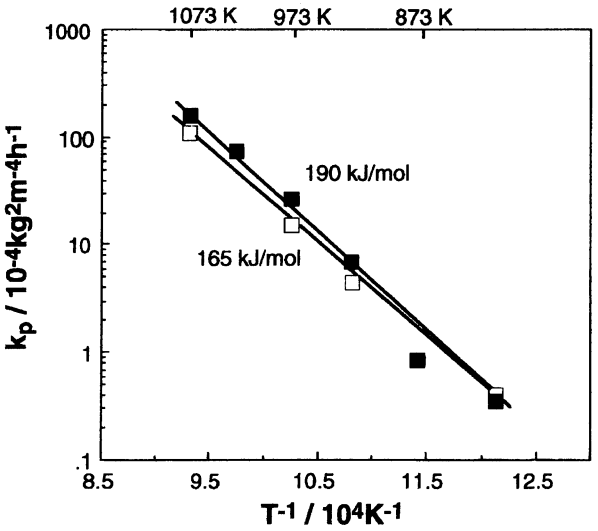

Fig. 5. Arrhenius plots of the parabolic rate constants (k_p) for the corrosion of Fe under $67\%CO_2$–$33\%O_2$. □: without melt, ■: coated with 35×10^{-2} kg m^{-2} of $(Li_{0.62}K_{0.38})_2CO_3$.

Figure 6 shows the relationship between the parabolic rate constant (k_p) of the corrosion of Fe coated with 32×10^{-2} kg m^{-2} of $(Li_{0.62}K_{0.38})_2CO_3$ and P_{CO_2} under $P_{O_2}=0.3$ atm at 923 K. The parabolic rate constants were independent of P_{co_2}. This means that CO_2 gas does not affect the corrosion reaction significantly.

Figure 7 shows the dependence of the parabolic rate constant for the corrosion of Fe coated with 32×10^{-2} kg m^{-2} of $(Li_{0.62}K_{0.38})_2CO_3$ on P_{O_2} under $P_{CO_2}=0.1$ atm at 923 K. The reaction obeyed the parabolic rate law and the parabolic rate constant decreased with increasing O_2 pressure. According to Wagner's theory,[11] the parabolic rate constant should increase or stay constant if the oxidant potential increases. The morphology or the composition of the oxide scale might be changed with an increase in the concentration of oxygen in the melt and the diffusion of the reaction species through the scale becomes more difficult at higher oxygen pressures.

Figure 8 shows the weight gain curves for the corrosion of Fe immersed in $(Li_{0.62}K_{0.38})_2CO_3$ under $33\%O_2$–$67\%CO_2$ at 823—1073 K (the weight ratio of Fe/melt=

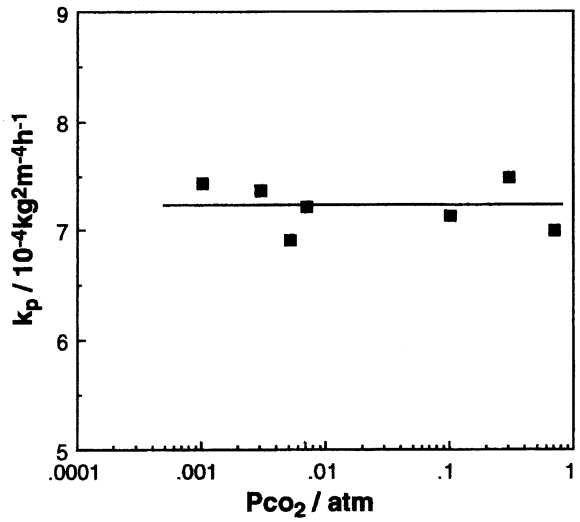

Fig. 6. Parabolic rate constant (k_p) for the corrosion of Fe coated with 32×10^{-2} kg m^{-2} of $(Li_{0.62}K_{0.38})_2CO_3$ vs. P_{CO_2} under $P_{O_2}=0.3$ atm at 923 K.

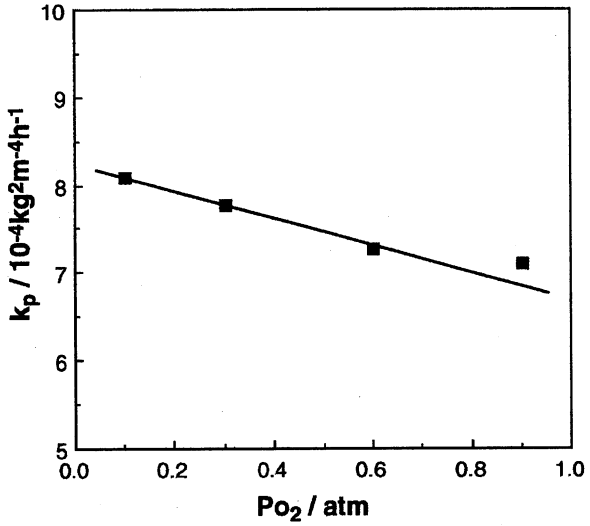

Fig. 7. Parabolic rate constant (k_p) for the corrosion of Fe coated with 32×10^{-2} kg m^{-2} of $(Li_{0.62}K_{0.38})_2CO_3$ vs. P_{O_2} under P_{CO_2}=0.1 atm at 923 K.

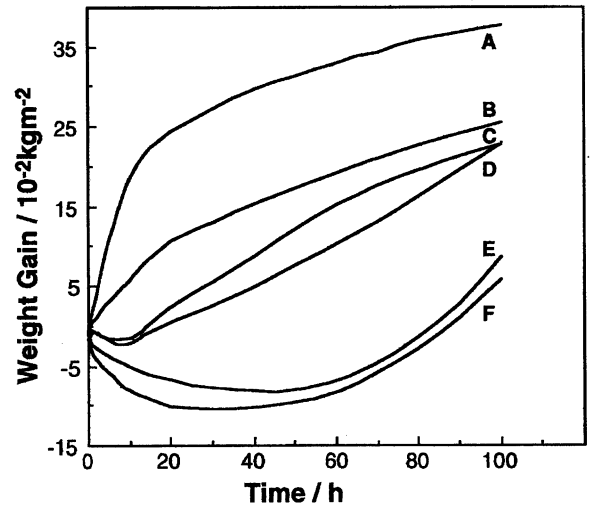

Fig. 8. Weight gain curves for the corrosion of Fe immersed in $(Li_{0.62}K_{0.38})_2CO_3$ under $67\%CO_2$–$33\%O_2$. Fe/melt=1/1.5. A: 823 K, B: 873 K, C: 923 K, D: 923 K, D: 973 K, E: 1023 K, F: 1073 K.

1/1.5). The weight increased from the initial period at 823 and 873 K. But the weight decreased during the initial period at 923—1073 K and then started to increase. The amount of weight decrease during the initial period increased with increasing temperature. If lithiated Fe oxide is formed, CO_2 gas is liberated from Li_2CO_3. This means the weight of a cell (specimen+melt) decreases, although the weight change depends on the Li content in the oxide scale.

After the immersion test at 923 and 1073 K, the corrosion products were analyzed by the X-ray diffraction method. Figure 9 shows the results. $LiFe_5O_8$ and $LiFeO_2$ were detected after 100 h for both temperatures (Fig. 9 (A) and (B)). However, the corrosion products

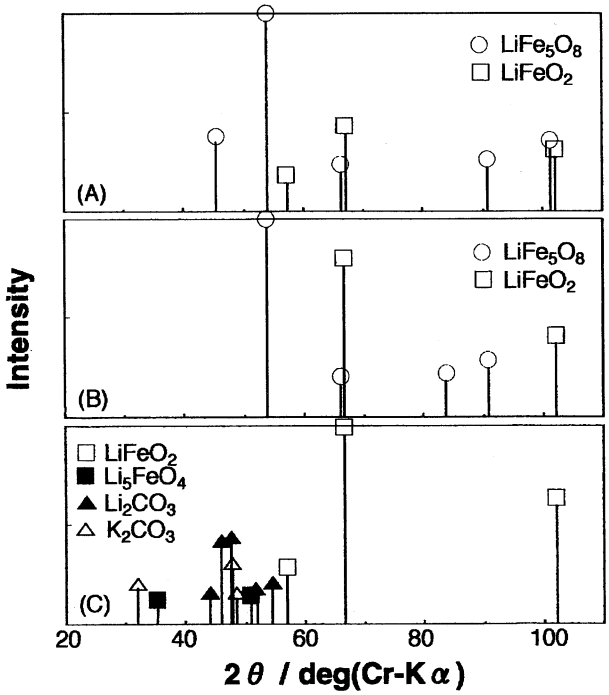

Fig. 9. X-Ray diffraction of the oxide scale of Fe corroded in $(Li_{0.62}K_{0.38})_2CO_3$ under $67\%CO_2$–$33\%O_2$. (A): at 923 K after 100 h, (B): at 1073 K after 100 h, (C): at 1073 K after 15 h. ■: Li_5FeO_4, □: $LiFeO_2$, ○: $LiFe_5O_8$, ▲: Li_2CO_3, △: K_2CO_3.

after 15 h at 1073 K were Li_5FeO_4 and $LiFeO_2$ (Fig. 9 (C)).

In order to measure the metal consumption during the corrosion reaction, the oxide scale was removed after the immersion test and the remaining Fe was weighed. Figure 10 shows the results of the metal consumption at 1073 K. The metal consumption linearly increased with time from the initial period of the reaction, although the weight of the cell (specimen+melt) decreased in the initial period. This means that the corrosion reaction of Fe in the carbonate melt obeys the linear rate law. Figure 11 shows the temperature dependence of the linear rate constant (k_l) calculated from the metal consumption at 100 h at each temperature. A linear correlation was seen with log k_l and $1/T$. This means that the corrosion reaction proceeded faster at higher temperatures, although the TGA of the cell (specimen+melt) showed a smaller weight gain at higher temperatures (Fig. 8).

Considering the reaction products, the corrosion reaction of Fe in the carbonate melt can be expressed as follows.

$$Fe + 1/2Li_2CO_3 + 3/4O_2 = LiFeO_2 + 1/2CO_2 \quad (1)$$

$$Fe + 1/10Li_2CO_3 + 3/4O_2 = 1/5LiFe_5O_8 + 1/10CO_2 \quad (2)$$

$$Fe + 5/2Li_2CO_3 + 3/4O_2 = Li_5FeO_4 + 5/2CO_2 \quad (3)$$

From these equations the weight changes of the cell (specimen+melt) can be calculated. When 1 mole of Fe

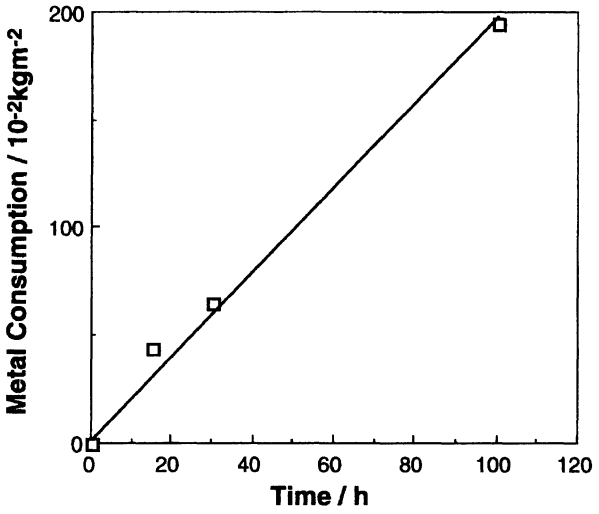

Fig. 10. Relation between metal consumption and reaction time in the corrosion of Fe immersed in $(Li_{0.62}K_{0.38})_2CO_3$ under 67%CO_2–33%O_2 at 1073 K. Fe/melt=1/1.5.

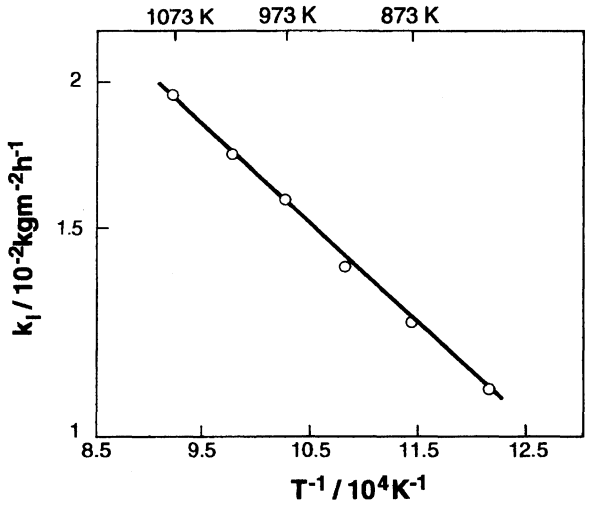

Fig. 11. Arrhenius plots for the linear rate constant (k_l) of the corrosion of Fe immersed in $(Li_{0.62}K_{0.38})_2CO_3$ under 67%CO_2–33%O_2.

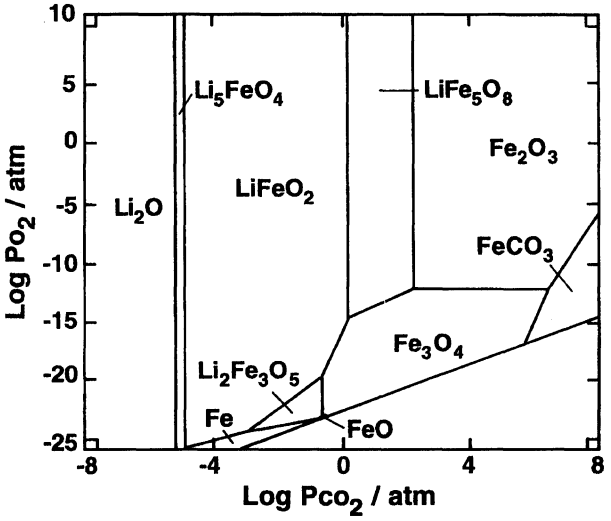

Fig. 12. Phase diagram of Fe in the Li–K–C–O system under CO_2–O_2 at 923 K. Activity of Li_2CO_3=0.2976, activity of K_2CO_3=0.0946.

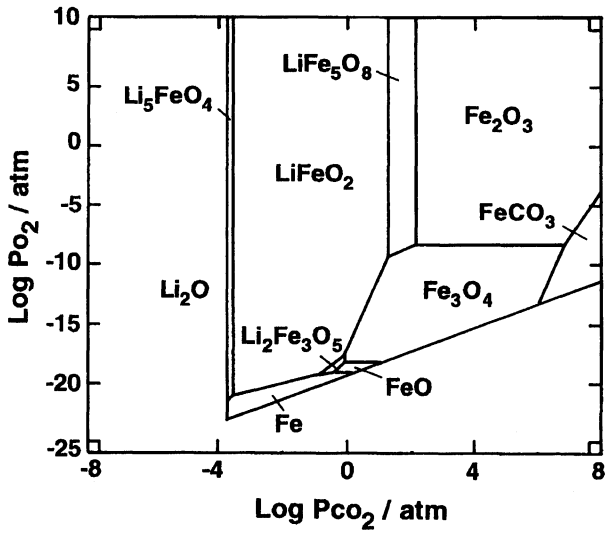

Fig. 13. Phase diagram of Fe in the Li–K–C–O system under CO_2–O_2 at 1073 K. Activity of Li_2CO_3= 0.2976, acitivity of K_2CO_3=0.0946.

is consumed by the corrosion reaction, the total weight change of the cell is 2, 19.6 and −86 g for Eqs. 1, 2, and 3, respectively. Li_5FeO_4 is the only compound that causes a weight decrease of the cell. Since the weight decrease of the cell was typically observed at higher temperatures, Li_5FeO_4 might be formed more easily at higher temperatures.

In order to estimate the corrosion product of Fe in the presence of $(Li_{0.62}K_{0.38})_2CO_3$, phase diagrams of the Li–K–Fe–C–O system were constructed.[12] Figures 12 and 13 show the phase diagrams of the Li–K–Fe–C–O system at 923 and 1073 K, where the activities of Li_2CO_3 and K_2CO_3 of the $(Li_{0.62}K_{0.38})_2CO_3$ melt were 0.2976 and 0.0946, respectively, which were obtained by Lessing.[14] From these phase diagrams, the possible corrosion products of Fe with the carbonate in this study are estimated to be $LiFe_5O_8$, $LiFeO_2$, and Li_5FeO_4. Although Fig. 13 is not so much different from Fig. 12, the stable region of $LiFeO_2$ in Fig. 13 moves to a higher CO_2 pressure. This means that $LiFe_5O_8$ is stable at 923 K in atmospheric pressure CO_2 and O_2, and Li_5FeO_4 is more likely to be formed at a higher temperature since the stable pressure region of CO_2 becomes higher. These considerations are consistent with the results of X-ray diffraction.

At 1073 K, Li_5FeO_4 was detected only in the initial period of the reaction. In other words, the formation of Li_5FeO_4 ceased in the later period. This can be explained by the decrease of Li in the oxide scale. As the

reaction proceeds, the Li content in the oxide decreases due to the formation of lithiated iron oxide. Figure 14 shows the phase diagram of the Li–K–Fe–C–O system when the activity of Li_2CO_3 is 10^{-4}. The stable region of Li_5FeO_4 shifted to extremely low CO_2 pressure which was lower than that at 923 K. Li_5FeO_4 is less likely to form under the conditions of Fig. 14 than Fig. 12 in a $67\%CO_2$–$33\%O_2$ atmosphere.

If the metal consumption and the weight increase of the cell are obtained, the metal consumption for each reaction product can be roughly calculated in the following way. At 1073 K, the reaction products were $LiFeO_2$ and Li_5FeO_4 during the initial period where the weight of the cell decreased. In Fig. 8, at 35 h the weight decrease reached a maximum and the metal consumption was 68.3×10^{-2} kg m^{-2} and the weight decrease of the cell was 10.4×10^{-2} kg m^{-2}. The following equation can thus be obtained.

$$W_{Fe}(LiFeO_2) + W_{Fe}(Li_5FeO_4) = 6.83 \times 10^{-2} g\,cm^{-2}, \quad (4)$$

where $W_{Fe}(LiFeO_2)$ and $W_{Fe}(Li_5FeO_4)$ denote the metal consumption per unit area due to the formation of $LiFeO_2$ and Li_5FeO_4, respectively. Taking into account Eqs. 1 and 3, the following equation is also obtained.

$$2W_{Fe}(LiFeO_2)/M_{Fe} - 86W_{Fe}(Li_5FeO_4)/M_{Fe} = -1.04 \times 10^{-2} g\,cm^{-2}, \quad (5)$$

where M_{Fe} is the molecular weight of Fe. From these equations, the metal consumption due to the formation of Li_5FeO_4 in the oxide scale was calculated to be 8.2×10^{-2} kg m^{-2} and that of $LiFeO_2$ was 60.2×10^{-2} kg m^{-2}.

After 35 h the weight of the cell increased. If we can assume that the formation of Li_5FeO_4 ceases after 35 h and $LiFeO_2$ and $LiFe_5O_8$ are formed, we can calculate the metal consumption due to the formation of $LiFeO_2$ and $LiFe_5O_8$. Figure 15 shows the results. The proportion of the metal consumption due to the formation of $LiFe_5O_8$ increases with time after 35 h. This tendency is consistent with that of the phase study (Fig. 14). At 100 h, the metal consumption due to the formation of Li_5FeO_4 is 4% of the total metal consumption. This amount is so small that the formation of Li_5FeO_4 could not be detected by X-ray diffraction.

Figure 16 shows the metal consumption for each of the reaction products which was calculated from the results of Figs. 8 and 11 in the same way at 923—1073 K. The metal consumption due to the formation of

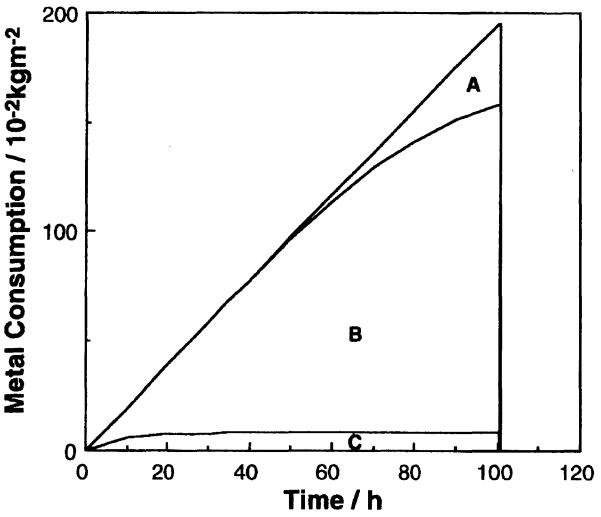

Fig. 15. Fe metal consumption in the corrosion of Fe immersed in $(Li_{0.62}K_{0.38})_2CO_3$ under $67\%CO_2$–$33\%O_2$ at 1073 K. A: $LiFe_5O_8$, B: $LiFeO_2$, C: Li_5FeO_4.

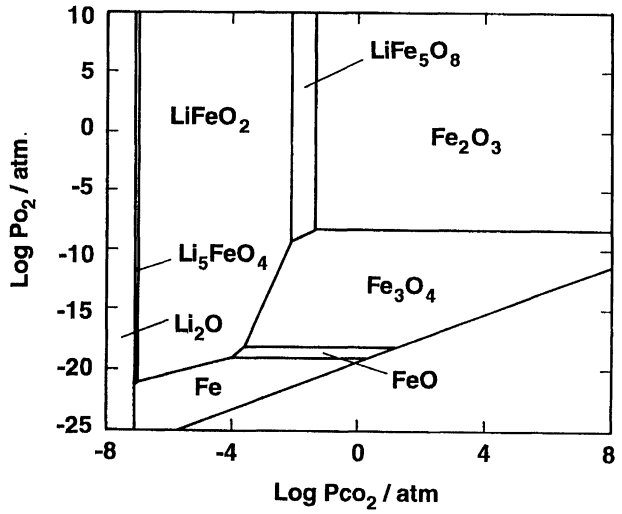

Fig. 14. Phase diagram of Fe in the Li–K–C–O system under CO_2–O_2 at 1073 K. Activity of $Li_2CO_3=10^{-4}$, activity of $K_2CO_3=0.0946$.

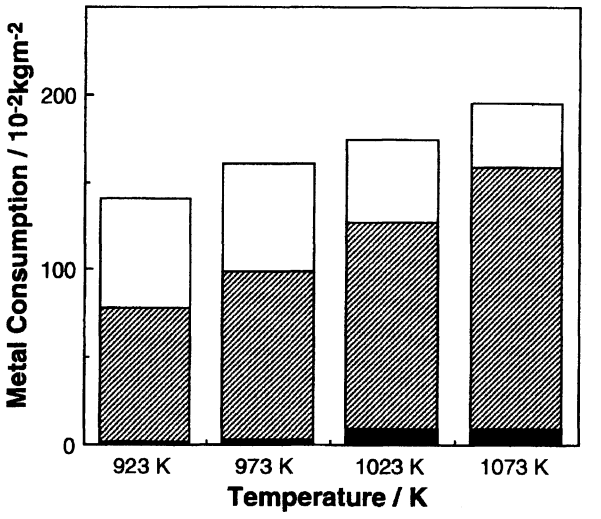

Fig. 16. Fe metal consumption in the corrosion of Fe immersed in $(Li_{0.62}K_{0.38})_2CO_3$ under $67\%CO_2$–$33\%O_2$. ■: Li_5FeO_4, ▨: $LiFeO_2$, □: $LiFe_5O_8$.

$LiFe_5O_8$ decreased at the higher temperature, while, the amount of metal consumption due to the formation of Li_5FeO_4 increased. These results are consistent with that of the phase diagram.

Conclusion

The corrosion of Fe in the presence of $(Li_{0.62}K_{0.38})_2CO_3$ was studied under a CO_2/O_2 atmosphere at 823—1073 K. The corrosion of Fe obeyed the parabolic rate law and the severe corrosion that usually takes place on Ni did not occur. Owing to the low solubility of iron oxide in the carbonate melt, the effect of the carbonate on the corrosion of Fe was small. In order to develop a stable alloy for the MCFC, iron-based alloys should be considered.

In this study, the weight change was monitored continuously by TGA. Therefore, the weight change of the reaction cell depended on the reaction products. Sometimes a weight decrease was observed, although the corrosion reaction proceeded. This point should be encountered if lithiated iron oxide is formed.

The authors express their thanks for the financial support of a Grant-in-Aid for Scientific Research from the Ministry of Education, Science and Culture.

References

1) D. A. Shores and P. Singh, in "Molten Carbonate Fuel Cell Technology," ed by J. R. Selman and T. D. Claar, The Electrochemical Society Softbound Proceeding Series, PV84-13, Pennington, NJ (1984), p. 271.
2) G. J. Janz and A. Conte, *Corrosion*, **20**, 237 (1984).
3) H. S. Hsu and J. H. DeVan, *J. Electrochem. Soc.*, **134**, 2077 (1984).
4) H. S. Hsu, J. H. DeVan, and M. Howell, *J. Electrochem. Soc.*, **134**, 3038 (1984).
5) S. Mitsushima, N. Kamiya, and K. Ota, *J. Electrochem. Soc.*, **137**, 2713 (1990).
6) G. Perzow, "Metallographisches Atzen," Translated by G. Matsumura, Agune, Japan (1977), p. 112.
7) K. Ota, B. Kim, H. Yoshitake, and N. Kamiya, in "Molten Salts," ed by R. J. Gale, G. Blomgren, and H. Kojima, The Electrochemical Society Softbound Proceeding Series, PV92-16, Pennington, NJ (1992), p. 162.
8) K. Ota, S. Mitsushima, K. Kato, and N. Kamiya, in "Molten Carbonate Fuel Cell Technology," ed by J. R. Selman, D. A. Shores, H. C. Maru, and I. Uchida, The Electrochemical Society Softbound Proceeding Series, PV90-16, Pennington, NJ (1990), p. 318.
9) K. Ota, B. Kim, H. Yoshitake, and N. Kamiya, *Bull. Chem. Soc. Jpn.*, submitted.
10) O. Kubaschewski and B. E. Hopkins, "Oxidation of Metals and Alloys," 2nd ed, Butterworths (1962), p. 270.
11) C. Wagner, "Atom Movement," Am. Soc. Met., Cleveland (1951), p. 158.
12) H. Yokokawa, N. Sakai, T. Kawada, M. Dokiya, S. Kato, and K. Ota, *Denki Kagaku*, **58**, 57 (1990).
13) D. F. Stull and H. Prophet, "JANAF Thermochemical Tables," 2nd ed, 10NSRDS-NBS37 (1971).
14) P. A. Lessing, Z. Z. Yang, G. R. Miller, and H. Yamada, *J. Electrochem. Soc.*, **135**, 1049 (1988).